

VALIDATION OF NEW SEMI-AUTOMATED ULTRASOUND IMAGE ANALYSIS METHOD FOR ASSESSING VASCULAR RESISTANCE IN MUSCULOSKELETAL TISSUES

Authors: Francisco J. Molina-Payá^{1*}, José Ríos-Díaz^{2*}, Francisco Carrasco-Martínez³, Jacinto J. Martínez-Payá⁴

Authors' affiliation:

¹ Department of Physiotherapy, Health Science Faculty, CEU-Cardenal Herrera University, CEU Universities, Elche (Spain) ORCID: 0000-0002-2343-3613. Email: clijamopa@gmail.com

² Escuela de Enfermería y Fisioterapia San Juan de Dios, Campus San Rafael, Universidad Pontificia de Comillas, Madrid (Spain). ORCID: 0000-0002-4786-3351. Email: jriofd@comillas.edu

³ Privace Practice. Clínica de fisioterapia F&C. Huelma (Spain) Email: clinicafcm@gmail.com

⁴ Physiotherapy Department, Facultad of Medicine, Universidad de Murcia, Murcia (Spain). ORCID: 0000-0002-9214-812X. Email: jmartinezpaya@um.es

Corresponding author: Campus San Rafael, Escuela de Enfermería y Fisioterapia San Juan de Dios, Universidad Pontificia de Comillas, Madrid (Spain). Paseo de la Habana 70 bis, Madrid, Spain

Email: jriofd@comillas.edu

Leve of evidence VI concurrent validity study

1 SUMMARY

1 **Objective:** The aim of this study was to analyze the concurrent validation between the resistance
2 index (RI) obtained by Spectral Doppler (SD) and the vascular resistance (VR) calculated by
3
4 quantifying pixel color intensity of the power Doppler (PD) signal.
5
6
7

8 **Methods:** The brachial artery of 30 healthy participants (24.8 yrs; SD = 6.44 yrs) were evaluated with
9 SD to automatically obtain RI and with PD to estimate de VR with de Pourcelot's formula from
10
11 systolic and diastolic peaks. Three assessments were performed on each participant, obtaining a total
12
13
14 of 90 ultrasound assessments of the brachial artery with their respective RI.
15
16
17

18 Processing and analysis were performed ImageJ software were manually selected and extracted from
19
20 the brachial artery PD images with the highest and lowest signal corresponding to peak systolic and
21
22
23 end diastole for each patient. The mean pixel color of the image with the highest signal was considered
24
25
26 as the peak systolic velocity and of the image with the lowest signal as the end-diastolic velocity.
27

28 **Results:** A high correlation was found between RI and VR ($r=.92$; 95%CI= .88 to .95; $p\leq .001$) so
29
30
31 there is a very strong concurrent validity between the two measures, and they can be considered
32
33
34 equivalentents (common variability of 84%).
35

36 **Conclusion:** This new method of analyzing DS by quantifying the color intensity of the PD signal
37
38 pixel is a good predictor of RI and could be useful for VR analysis in musculoskeletal tissues where
39
40
41 measurement of RI is complicated such in neovascularization in tendinopathies with multiple Doppler
42
43
44 signals.
45

46 **KEYWORDS:** Image Analysis; Musculoskeletal vascularization; Power-Doppler Ultrasonography;
47
48 Resistance Index; Vascular Resistance
49

50

51

52

53

54

55

56

57

58

59

60

61

62

63

64

65

23 1. INTRODUCTION

1
24 The use of Doppler ultrasound in the assessment of musculoskeletal pathologies is becoming
3
45 increasingly common (1,2). Doppler ultrasound can be used to localize areas of increased blood flow
5
6 and quantify color pixels, which can provide clinically important information, more accurate
7
8 diagnoses, and assessments of response to treatment (3). In tendinopathies, it allows locating areas
9
10 with intratendinous Doppler signal (IDS) (4), although we must keep in mind that the presence of
11
12 IDS does not provide relevant data about the tendinopathy (5,6). However, the study of vascular
13
14 resistance (VR) could provide more useful information on tissue status (7,8).
15
16

17
18 Currently, the pathophysiological model of the continuous model of tendinopathy is assumed
19
20 (9), in which the degenerative and reactive process coexist (10), and although this model makes little
21
22 reference to inflammation, some studies have observed a coexistence of inflammatory and
23
24 degenerative processes in the development of tendinopathies (7,11,12).
25
26

27
28 Spectral Doppler allows assessment of the type of blood flow, low or high resistance, by
29
30 means of a velocity versus time curve that represents the variation of red blood cell flow velocity
31
32 throughout the cardiac cycle. Spectral Doppler can be used to measure the degree of resistance to
33
34 arterial flow originating from the distal microvascular bed, expressed numerically with the resistance
35
36 index (RI). On a musculoskeletal level, a RI equal to 1 is considered normal, while a lower value
37
38 could be associated with inflammatory processes (7,13,14). The RI is provided directly by spectral
39
40 Doppler ultrasound from the Pourcelot formula: $[\text{peak systolic velocity} - \text{end-diastolic velocity}] /$
41
42 $[\text{peak systolic velocity}]$ (15).
43
44

45
46 For this purpose, the Doppler window is adjusted longitudinally, centered on the vessel lumen
47
48 and occupying 2/3 of its section. IDS seen in tendinopathies may contain vessels with a smaller lumen
49
50 than the Doppler window, so in many cases it is not possible to adjust the Doppler window to the size
51
52 of these vessels. In addition, many IDS may appear, complicating and multiplying the measurement
53
54 process in the attempt to obtain the mean RI of the IDS.
55
56
57
58
59
60
61
62
63
64
65

48 To avoid this problem, some authors have proposed to measure the RI in the three
1
2 49 intratendinous vessels with the largest diameter and to calculate the mean (13,14,16) but the large
3
4 50 number of intratendinous vessels that can be found suggests that this methodology is probably not
5
6 51 adequate enough to reproduce the entire intratendinous vascular resistance.

8
9 52 The analysis of the IDS through the color pixels not only allows quantification of the area of
10
11 53 the Spectral Doppler (17), but also **the establishment** of a relationship between pixel color intensity
12
13
14 54 scale and flow velocity (18), so it could be used to measure the intratendinous vascular resistance
15
16 55 through the resistance index formula. **Contrary to the RI measurement**, this procedure would allow
17
18 56 its application on any number and size of IDS found within the Doppler window.

20
21 57 Although the intra- and **inter**-observer reliability of selection and quantification in Power
22
23 58 Doppler mode has already been demonstrated(19), there are no studies that have analyzed the
24
25
26 59 relationship between the RI provided directly by the ultrasonographic device and that estimated from
27
28 60 the intensity of the color pixels. The consistent validity of the latter method would allow its
29
30
31 61 application in tendon hypervascularization.

32
33 62 The aim of this study was to analyze the concurrent validation between the resistance index
34
35
36 63 obtained by spectral Doppler and the vascular resistance calculated by quantifying pixel color
37
38 64 intensity of the power Doppler signal.

40 65 **2. MATERIALS AND METHODS**

42 66 **2.1. Study design and participants**

44
45 67 A total of 30 healthy participants with a systolic blood pressure lower than 130 mmHg and
46
47
48 68 diastolic blood pressure lower than 80 mmHg and no medical history of pathologies or medication
49
50 69 that could alter blood flow were included for this study. Participants were recruited voluntarily at a
51
52
53 70 private physiotherapy center (**Clinica F&C Fisioterapia Avanzada y Neurorehabilitación, Huelma,**
54
55 71 **Spain) in December 2018.** All participants were informed about the study and signed an informed
56
57
58 72 consent document. The study was approved by the Ethics Committee of the Catholic University of
59
60 73 Murcia (CE111803) **and follows the rules of Muscles, Ligaments and Tendons Journal (MLTJ) (20).**

74 2.2. Power Doppler and Spectral Doppler evaluation

1
275 The patient was placed in supine decubitus with the right upper limb in a comfortable position
3
476 to image the brachial artery.

677 The brachial artery was chosen to test the two methods because measurement of the RI in the
8
978 brachial artery does not offer difficulties, since it is a single vessel with a large lumen diameter and
10
1179 allows automatic acquisition of this index by the ultrasound scanner itself. In addition, the RI of the
12
13
1480 brachial artery is easily modified by vascular occlusion maintained for 5 min, which will generate
15
1681 hyperemia at 1 min after occlusion, with a decrease in RI (21). In other words, vascular occlusion of
17
18
1982 the brachial artery allows alteration of the RI recordings, decreasing its value to test the two methods
20
2183 in different situations.

2384 The examination was performed with two Telemed SmartUS ultrasound scanners (Vilnius,
24
25
2685 Lithuania) with 7-15 MHz linear transducers (L15-7L40H-5) and a Riester Minimus III pressure cuff
27
2886 (Jungingen, Germany) placed on the most distal part of the participant's arm (22–24).

30
3187 One of the transducers was installed on an articulated arm to maintain its static position on
32
3388 the longitudinal plane of the brachial artery at the midpoint between the antecubital and axillary
34
35
3689 regions. The ultrasound machine, in spectral Doppler mode, identified the cardiac cycles, as well as
37
3890 the peak systolic velocity and end-diastolic velocity, automatically calculating the RI of the brachial
39
40
4191 artery.

42
4392 The second transducer was placed distal to the first and transversal to the brachial artery to
44
45
4693 record the PD. A Doppler frequency of 6.7 MHz and a pulse repetition frequency of 1.5 kHz were
47
4894 used. The lowest wall filter and standardized gain were applied just below the level that produced
49
5095 random noise. The setting parameters were the same for all patients and minimal pressure was exerted
51
52
5396 with the transducer on the arm to avoid vessel compression.

54
5597 Brachial artery occlusion was applied for 5 min distal to the ultrasound slices with the pressure
56
57
5898 cuff, using a pressure calculated from the systolic arterial pressure + 50 mmHg (23,25). In this way,

99 endothelium-mediated, nitric oxide-dependent ischemia and subsequent reactive hyperemia were
100 induced.

101 At 1 min post-occlusion and coinciding with the vasodilatation generated by hyperemia and
102 therefore a decrease in the RI (21,26,27), the RI and a 4 seconds video of the transverse PD signal to
103 the brachial artery were recorded by the two ultrasound scanners at the same time. The location of
104 the ultrasound transducers and pressure cuff can be seen in **figure 1**.

105 Three assessments were performed on each participant, obtaining a total of 90 ultrasound
106 assessments of the brachial artery with their respective RI and 4 seconds videos of the PD signal after
107 vascular occlusion. All scans were performed by the same sonographer with more than 15 years of
108 experience in musculoskeletal ultrasound.

109 **2.3. Quantification of intratendinous vascular resistance with Doppler Ultrasonography**

110 Processing and analysis of the videos and images were performed by a second investigator
111 using ImageJ software (Version 1.50b, National Institutes of Health, Bethesda, MD, USA). After
112 image scaling, regions of interest (ROI) were manually selected and extracted from the brachial artery
113 PD images with the highest and lowest signal corresponding to peak systolic and end diastole for each
114 patient. Measurement and image data were coded and anonymized to avoid potential bias.

115 Since the IDS appears in color on a grayscale background, it is easy to segment and isolate
116 the region for further quantification. We used the color threshold plug-in, which allows the cutoff
117 point to be manually adjusted with slider bars.

118 The flow pattern was assessed by calculating the mean pixel color intensity of the previously
119 isolated PD signal for each image. The mean pixel color of the image with the highest signal was
120 considered as the peak systolic velocity and of the image with the lowest signal as the end-diastolic
121 velocity. These data were transferred to the RI formula, giving a value associated with the RV of the
122 brachial artery (**figure 2**). The reproducibility and reliability of this procedure has been previously
123 studied in IDS(19) with a very good intra- and interobserver agreement (ICC = .92; 95% IC = .86 to
124 .96).

125 **2.4. Sample size**

126 This study has an exploratory aim, so a sample of 30 healthy participants were recruited in a
127 non-random, purposive, and consecutive manner.

128 **2.5. Statistical methods**

129 Data analysis was conducted with the statistical package R v.3.6 and JASP Team (2020).
130 JASP (Version 0.14.1) [Computer software].

131 Data were summarized using mean and standard deviation and range and quartiles for
132 continuous variables and absolute and relative frequencies for categorical variables.

133 Although the sample size allows the assumption of normality, multivariate and bivariate
134 normality was explored with the Shapiro-Wilks test; in all contrasts the W statistic was near to 1.0,
135 so the assumption of normality was finally assumed.

136 Correlation was assessed with Pearson's r correlation coefficient (95% CI) and the percentage
137 of shared variability between pairs of variables was determined with the coefficient of determination
138 ($r^2\%$). In addition, the Vovk-Sellke Maximum p -Ratio was estimated, which provides the degree of
139 plausibility evidence for the alternative hypothesis (presence of correlation), compared to the null
140 hypothesis (no correlation), regardless of the p -values(28).

141 As a guideline, the following cut-off points will be considered for correlations: .0 to .19 - very
142 weak correlation; .2 to .39 - weak correlation; .4 to .69 - moderate correlation; .7 to .89 - strong
143 correlation; .9 to 1.0 - very strong correlation. In all cases, the significance level was set at $p \leq .05$.

144 **3. RESULTS**

145 Thirty participants (16 women [53%], mean age = 24.8 years; SD = 6.44 years) were included
146 in this study. A descriptive summary of variables is shown in **table I**.

147 The correlations between variables of interest obtained from IDS, RI and VR are shown in
148 **table II**, and **figure 3**.

149 Ahigh correlation was found between RI and VR ($r=.92$; 95%CI= .88 to .95; $p\leq .001$) so there
150 is a very strong concurrent validity between the two measures, and they can be considered equivalents
151 (common variability of 84%).

152 We found interesting moderate correlations between the Doppler area at the systolic peak with
153 respect to IR ($r=.53$; 95%CI= .36 to .67; $p\leq .001$) and RV ($r=.57$; 95%CI= .41 to .69; $p\leq .001$) in a
154 similar way, but no correlation with respect to the area in diastole.

155 Similarly, a strong correlation was found between the mean intensity of color pixels in systole
156 with respect to RI ($r=.72$; 95%CI= .61 to .81; $p\leq .001$) and RV ($r=.85$; 95%CI= .78 to .90; $p\leq .001$)
157 but not with respect to diastole.

158 **4. DISCUSSION**

159 No other studies have been found that correlate RI with other methods of measuring VR, so
160 the results obtained cannot be compared. Regarding the correlation between VR calculated by
161 quantifying the color intensity of the pixels of the PD signal and the RI measured at the same time
162 and over the brachial artery, it was observed that there is a positive correlation, that is, the higher the
163 value of VR, the higher the RI.

164 It is difficult to think that the mean raw pixel color of the PD signal correlates with the flow
165 velocity, because there are different filtering and interpolarization algorithms to represent the image
166 that can distort the results. Moreover, this study used the PD mode, which encodes the amplitude of
167 the signal by the number of red blood cells that are moving, which provides information on the
168 amplitude of the IDS, as opposed to Color Doppler which encodes the average of the velocities.

169 This issue could further complicate this correlation because the RI is calculated with flow
170 velocity data and the PD provides information on intensity. Although the results obtained in this study
171 have been very good, it would be interesting to study the correlation of this methodology applied on
172 the color IDS. However, in relation to the RI and given that it is a relative index, it seems that the two
173 types of measures are equivalent.

174 In 1995, Delorme studied the relationship between the mean pixel color of the color Doppler
175 and flow velocity (18). The limitations of this modality of ultrasound are related to the interpolation
176 algorithms used by the ultrasound machine itself when low levels of color Doppler are used, giving
177 erroneous low values for the mean pixel color value. The selection of an inadequate velocity scale
178 and insonation angle in the color Doppler mode can generate aliasing (29), altering the color
179 representation of the signal pixel. Despite these limitations, the use of average pixel color analysis of
180 the color Doppler is applicable in practice and provides additional information in the assessment of
181 IDS (18).

182 Although the quantification of the color IDS has been extensively studied (18,30,31),
183 quantification of PD signals has several advantages over color Doppler in the assessment of tissue
184 vascularization and blood flow. In the case of this study, the PD mode has been used because it is less
185 dependent on the Doppler angle, it is more sensitive in the representation of low flows in small
186 vessels, aliasing does not appear (32), and the codification in a single color tone facilitates the
187 quantification process and the results obtained correlate well with the perfusion rate (33).

188 *Limitations*

189 This quantification methodology has some limitations, mainly related to standardization, as it
190 depends on the sensitivity and color tone of the PD signals, which are altered by different parameters
191 such as: the ultrasound model and transducer used, the selection of ultrasound slices, the selection of
192 images with higher and lower IDS from the video sequence, the settings of the ultrasound Doppler
193 parameters, the color scale used, the delimitation of the ROI of the IDS in the image and the manual
194 selection of the color thresholds of the image analysis software. However, in this study all these
195 parameters have been optimized and kept constants for all scans.

196 **5. CONCLUSION**

197 As conclusion, our method of analysing intratendinous Doppler signal by quantifying the
198 colour intensity of the Power Doppler signal pixel is a good predictor of resistance index and could

199 be useful for vascular resistance analysis in tissues where measurement of resistance index is
200 complicated as in tendinopathies.

1
2
3
4
5
6
7

202 **Funding:** This research did not receive any specific grant from funding agencies in the
203 public, commercial, or not-for-profit sectors.

8
9
10
11
12

204 **Conflict of interest:** The authors declare no conflicts of interest

13
14
15

205 **Author's contribution:** FJMP and JRD contribute equally. JJMP and FMC took the
206 images. FJMP processed and analyzed videos and images. JRD processed and analyzed data. FJMP
207 and JRD wrote the manuscript. All authors revised and approved the final version of manuscript

18
19
20
21
22

23
24
25
26
27
28
29
30
31
32
33
34
35
36
37
38
39
40
41
42
43
44
45
46
47
48
49
50
51
52
53
54
55
56
57
58
59
60
61
62
63
64
65

209 **6. REFERENCES**

- 1
210 1. Mersmann F, Pentidis N, Tsai MS, Schroll A, Arampatzis A. Patellar Tendon Strain
211 Associates to Tendon Structural Abnormalities in Adolescent Athletes. *Front Physiol.*
212 2019;10:963.
5
- 213 2. Risch L, Stoll J, Schomöller A, Engel T, Mayer F, Cassel M. Intraindividual Doppler Flow
214 Response to Exercise Differs Between Symptomatic and Asymptomatic Achilles Tendons.
215 *Front Physiol.* 2021;12:617497.
7
8
- 10
1216 3. McCreesh KM, Riley SJ, Crotty JM. Neovascularity in patellar tendinopathy and the response
1217 to eccentric training: a case report using Power Doppler ultrasound. *Man Ther.*
1218 2013;18(6):602-5.
13
14
- 15
1219 4. Gatz M, Betsch M, Bode D, Schweda S, Dirrichs T, Migliorini F, et al. Intra individual
1220 comparison of unilateral Achilles tendinopathy using B-mode, power Doppler, ultrasound
1221 tissue characterization and shear wave elastography. *J Sports Med Phys Fitness.*
1222 2020;60(11):1462-9.
19
20
- 21
223 5. Malliaras P, Richards PJ, Garau G, Maffulli N. Achilles tendon Doppler flow may be
224 associated with mechanical loading among active athletes. *Am J Sports Med.*
225 2008;36(11):2210-5.
25
- 26
226 6. Tol JL, Spiezia F, Maffulli N. Neovascularization in Achilles tendinopathy: have we been
227 chasing a red herring? *Knee Surg Sports Traumatol Arthrosc Off J ESSKA.*
228 2012;20(10):1891-4.
29
30
- 329 7. Torp-Pedersen TE, Torp-Pedersen ST, Qvistgaard E, Bliddal H. Effect of glucocorticosteroid
330 injections in tennis elbow verified on colour Doppler ultrasonography: evidence of
331 inflammation. *Br J Sports Med.* 2008;42(12):978-82.
34
- 35
332 8. Terabayashi N, Watanabe T, Matsumoto K, Takigami I, Ito Y, Fukuta M, et al. Increased
333 blood flow in the anterior humeral circumflex artery correlates with night pain in patients with
334 rotator cuff tear. *J Orthop Sci Off J Jpn Orthop Assoc.* 2014;19(5):744-9.
39
- 40
235 9. Cook JL, Purdam CR. Is tendon pathology a continuum? A pathology model to explain the
41 clinical presentation of load-induced tendinopathy. *Br J Sports Med.* 2009;43(6):409-16.
42
- 43
437 10. Cook JL, Rio E, Purdam CR, Docking SI. Revisiting the continuum model of tendon
438 pathology: what is its merit in clinical practice and research? *Br J Sports Med.*
439 2016;50(19):1187-91.
47
- 48
240 11. Chisari E, Rehak L, Khan WS, Maffulli N. Tendon healing is adversely affected by low-grade
49 inflammation. *J Orthop Surg.* 4 de diciembre de 2021;16(1):700.
51
- 5242 12. D'Addona A, Maffulli N, Formisano S, Rosa D. Inflammation in tendinopathy. *Surg J R Coll
5243 Surg Edinb Irel.* octubre de 2017;15(5):297-302.
54
- 55
5244 12. Koenig MJ, Torp-Pedersen S, Holmich P, Terslev L, Nielsen MB, Boesen M, et al. Ultrasound
5245 Doppler of the Achilles tendon before and after injection of an ultrasound contrast agent--
5246 findings in asymptomatic subjects. *Ultraschall Med.* 2007;28(1):52-6.
59

- 247 13. Koenig MJ, Torp-Pedersen ST, Christensen R, Boesen MI, Terslev L, Hartkopp A, et al.
248 Effect of knee position on ultrasound Doppler findings in patients with patellar tendon
249 hyperaemia (jumper's knee). *Ultraschall Med.* 2007;28(5):479-83.
- 250 14. Pourcelot L. Application de l'examen Doppler à l'étude de la circulation périphérique. Paris:
251 Éditions médicales Spécia; 1982.
- 252 15. Qvistgaard E, Røgind H, Torp-Pedersen S, Terslev L, Danneskiold-Samsøe B, Bliddal H.
253 Quantitative ultrasonography in rheumatoid arthritis: evaluation of inflammation by Doppler
254 technique. *Ann Rheum Dis.* 2001;60(7):690-3.
- 1255 16. Rezaei H, af Klint E, Hammer HB, Terslev L, D'Agostino MA, Kisten Y, et al. Analysis of
1256 correlation and causes for discrepancy between quantitative and semi-quantitative Doppler
1257 scores in synovitis in rheumatoid arthritis. *Rheumatol Oxf Engl.* 2017;56(2):255-62.
- 1258 17. Delorme S, Weisser G, Zuna I, Fein M, Lorenz A, van Kaick G. Quantitative characterization
1259 of color Doppler images: reproducibility, accuracy, and limitations. *J Clin Ultrasound.*
1260 1995;23(9):537-50.
- 21 19. Molina-Payá FJ, Ríos-Díaz J, Carrasco-Martínez F, Martínez-Payá JJ. Reliability of a New
22 Semi-automatic Image Analysis Method for Evaluating the Doppler Signal and Intratendinous
23 Vascular Resistance in Patellar Tendinopathy. *Ultrasound Med Biol.* diciembre de
24 2021;47(12):3491-500.
- 25 20. Ethics Approval For Papers Submitted To "Muscles, Ligaments And Tendons Journal" –
26 MLTJ [Internet]. [citado 9 de septiembre de 2022]. Disponible en:
27 <http://www.mltj.online/ethical-policies-of-muscle-ligaments-and-tendons-journal/>
- 31 19. Takarada Y, Takazawa H, Sato Y, Takebayashi S, Tanaka Y, Ishii N. Effects of resistance
32 exercise combined with moderate vascular occlusion on muscular function in humans. *J Appl*
33 *Physiol.* 2000;88(6):2097-106.
- 34 20. Frangi AF, Laclaustra M, Lamata P. A registration-based approach to quantify flow-mediated
35 dilation (FMD) of the brachial artery in ultrasound image sequences. *IEEE Trans Med*
36 *Imaging.* 2003;22(11):1458-69.
- 37 21. Harris RA, Nishiyama SK, Wray DW, Richardson RS. Ultrasound assessment of flow-
38 mediated dilation. *Hypertens Dallas Tex.* 2010;55(5):1075-85.
- 39 22. Wray DW, Witman MAH, Ives SJ, McDaniel J, Trinity JD, Conklin JD, et al. Does brachial
40 artery flow-mediated vasodilation provide a bioassay for NO? *Hypertens Dallas Tex.*
41 2013;62(2):345-51.
- 42 23. Corretti MC, Anderson TJ, Benjamin EJ, Celermajer D, Charbonneau F, Creager MA, et al.
43 Guidelines for the ultrasound assessment of endothelial-dependent flow-mediated vasodilation
44 of the brachial artery: a report of the International Brachial Artery Reactivity Task Force. *J*
45 *Am Coll Cardiol.* 2002;39(2):257-65.
- 46 24. Betik AC, Luckham VB, Hughson RL. Flow-mediated dilation in human brachial artery after
47 different circulatory occlusion conditions. *Am J Physiol Heart Circ Physiol.*
48 2004;286(1):H442-448.

- 286 25. Rafati M, Mokhtari-Dizaji M, Saberi H. The Effect of Cuff Occlusion Protocols on Radial
287 Strain and Arterial Haemodynamics. *Ultrasound*. 2009;17(3):144-9.
1
- 288 28. Sellke T, Bayarri MJ, Berger JO. Calibration of p Values for Testing Precise Null Hypotheses.
289 *Am Stat*. 55(1):62-71.
3
- 290 27. SEUS, Sánchez Guerrero Á, Del Cura Rodríguez JL. *Ecografía Doppler Esencial*. Madrid:
291 Médica Panamericana; 2021
5
- 292 30. Bell DS, Bamber JC, Eckersley RJ. Segmentation and analysis of colour Doppler images of
10 tumour vasculature. *Ultrasound Med Biol*. 1995;21(5):635-47.
14
- 294 31. Fein M, Delorme S, Weisser G, Zuna I, van Kaick G. Quantification of color Doppler for the
14 evaluation of tissue vascularization. *Ultrasound Med Biol*. 1995;21(8):1013-9.
15
- 296 32. Pozniak MA, Allan PL. *Clinical Doppler Ultrasound E-Book: Expert Consult: Online*. Elsevier
17 Health Sciences; 2013. 401 p.
18
- 298 31. Sehgal CM, Arger PH, Silver AC, Patton JA, Saunders HM, Bhattacharyya A, et al. Renal
21 blood flow changes induced with endothelin-1 and fenoldopam mesylate at quantitative
22 Doppler US: initial results in a canine study. *Radiology*. 2001;219(2):419-26.
23

24
25
26
27
28
29
30
31
32
33
34
35
36
37
38
39
40
41
42
43
44
45
46
47
48
49
50
51
52
53
54
55
56
57
58
59
60
61
62
63
64
65

303 **Figure 1.** Location of ultrasound transducers and pressure cuff.

1
304 **Figure 2.** Quantification of vascular resistance by pixel color intensity from Power Doppler
2
3
305 video with Doppler signal processing and calculation of mean of mean color pixels.
4
5

6
306 **Figure 3.** Regression lines between RI, VR, and systolic parameters and Pearson's r heatmap.
7
8
307 RI: resistance index. VR: vascular resistance. SPV. px: mean of color pixel in systolic peak velocity.
9
10

11
308
12
13
14
15
16
17
18
19
20
21
22
23
24
25
26
27
28
29
30
31
32
33
34
35
36
37
38
39
40
41
42
43
44
45
46
47
48
49
50
51
52
53
54
55
56
57
58
59
60
61
62
63
64
65

Figure 1

[Click here to access/download;Figures;Figure 1.tif](#)



Figure 2

[Click here to access/download;Figures;Figure 2.tif](#)

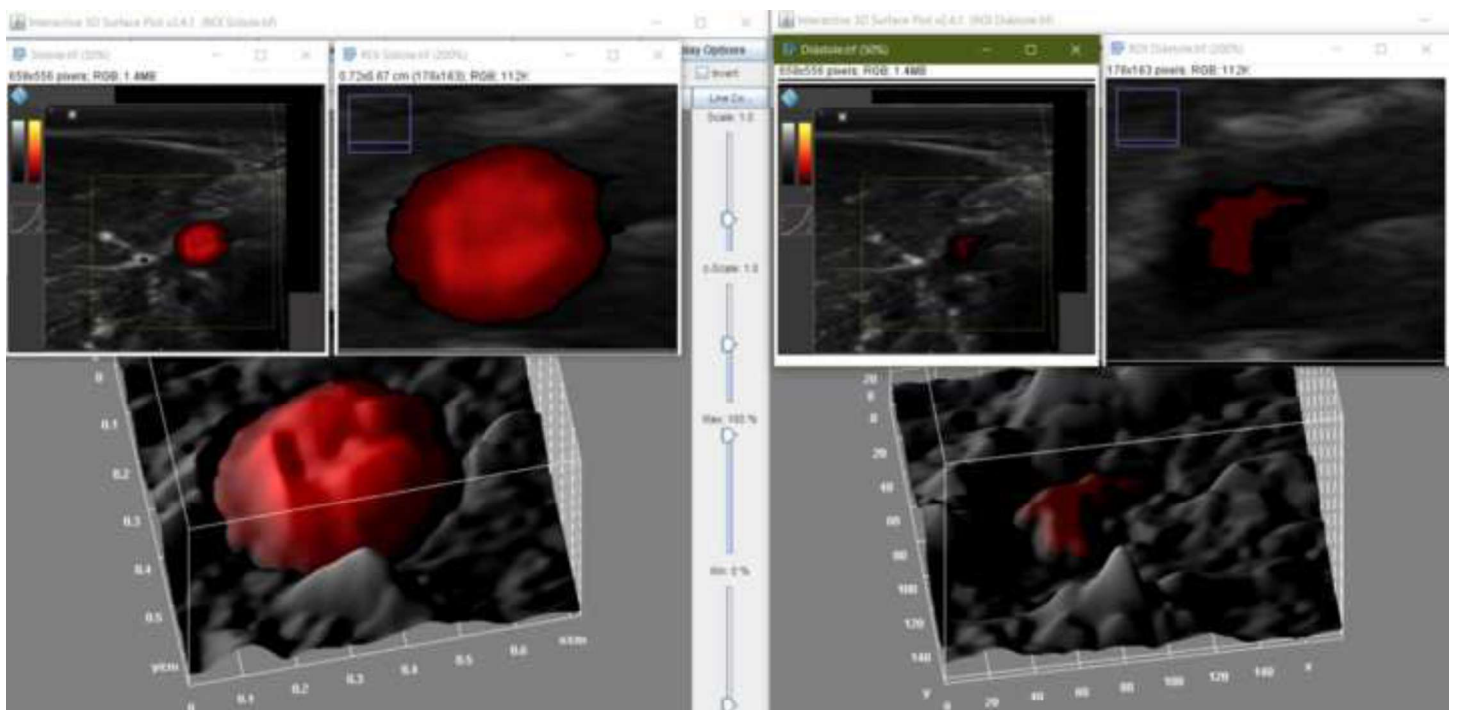


Imagen2.svg

Figure 3

[Click here to access/download;Figures;Figure 3.tif](#)

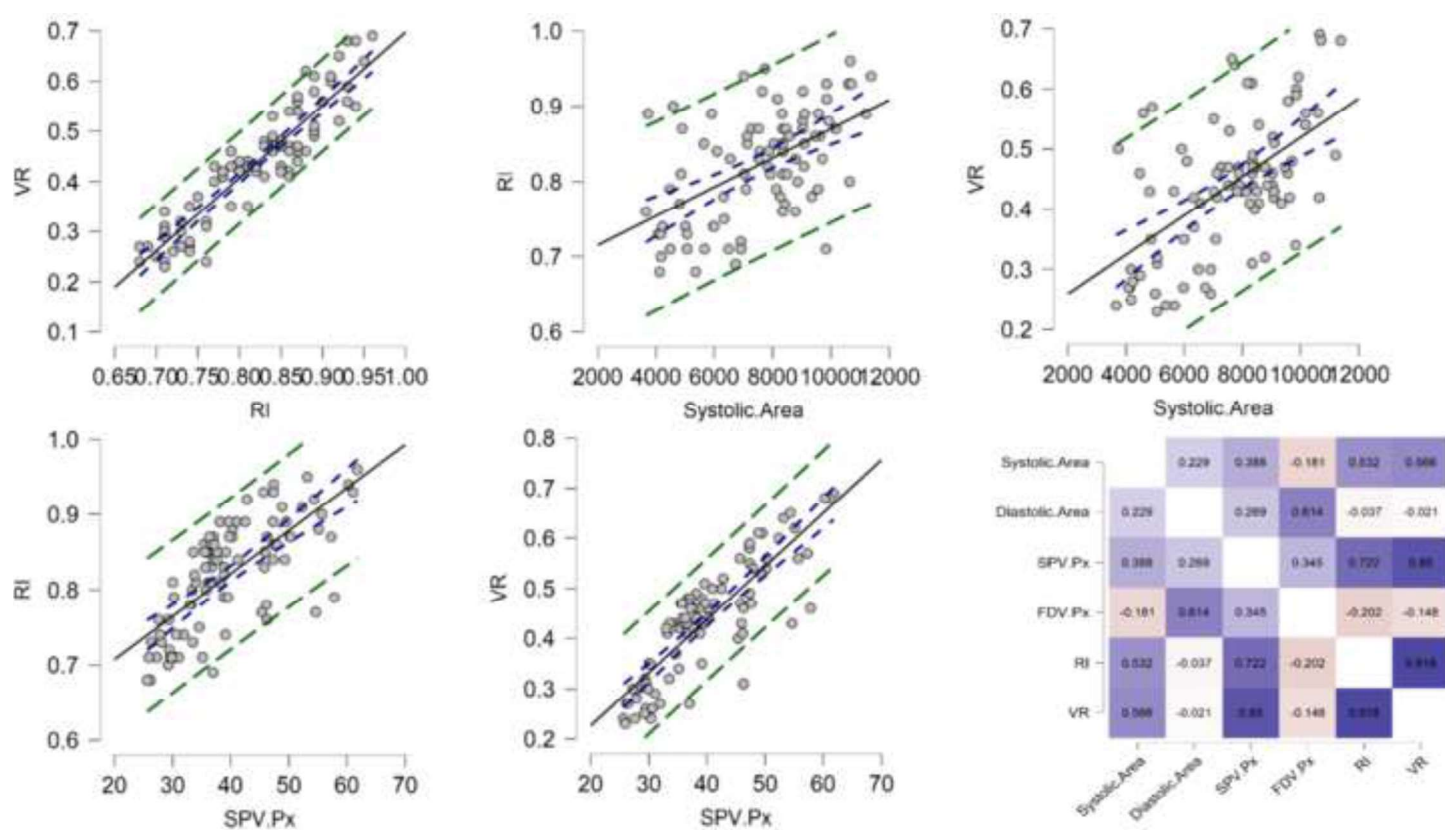


Table I. Descriptive summary of Doppler parameters.

Parameter	Mean	SD	VC%	Min	Q1	Median	Q3	Max
Area SPV	7520.1	1997.56	27%	3656.0	5980.5	7877.5	9037.0	11383.0
Area FDV	2328.4	1222.99	53%	268.0	1493.3	2152.0	3035.5	6356.0
Color pixel intensity SPV	40.1	9.18	23%	25.7	33.5	38.2	47.1	61.8
Color pixel intensity FDV	21.6	2.75	13%	19.0	19.5	20.8	22.7	31.7
Resistance index	0.82	0.073	9%	0.68	0.76	0.84	0.87	0.96
Vascular resistance	0.44	0.115	26%	0.23	0.35	0.44	0.50	0.69

SPV: Systolic Peak velocity. FDV: final diastolic velocity. SD: Standard deviation. VC%: variation coefficient. Q1: quartile 1. Q2: quartile 2. Min: minimum. Max: Maximum.

Table II. Pairwise correlations between PD color variables and RI.

Pairwise correlation	Pearson's r (95%CI)	p-value	R²%	VS-MPR
RI-VR	.92 (.88 to .95)	≤.001	84%	≥300
Systolic Area-SPV.px	.39 (.2 to .55)	≤.001	15%	262
Systolic Area-FDV.px	-.18 (-.37 to .03)	.09	3%	1.7
Systolic Area-RI	.53 (.36 to .67)	≤.001	28%	≥300
Systolic Area-VR	.57 (.41 to .69)	≤.001	32%	≥300
Diastolic Area-SPV.px	.27 (.07 to .45)	.010	7%	7.8
Diastolic Area-FDV.px	.61 (.47 to .73)	≤.001	38%	≥300
Diastolic Area-RI	-.04 (-.24 to .17)	.073	0%	1.0
Diastolic Area-VR	-.02 (-.23 to .19)	.85	0%	1.0
SPV.Px-RI	.72 (.61 to .81)	≤.001	52%	≥300
SPV.Px-VR	.85 (.78 to .9)	≤.001	72%	≥300
FDV.Px-RI	-.2 (-.39 to .01)	.06	4%	2.3
FDV.Px-VR	-.15 (-.34 to .06)	0.16	2%	1.2

RI: resistance index. VR: vascular resistance. SPV.px: mean color pixel intensity in systolic peak of velocity. FDV.px: mean color pixel intensity in final diastolic velocity. Vovk-Sellke Maximum p-Ratio: Based on the p-value, the maximum possible odds in favor of H1 over H0 equals $1/e^{-p} (\log(p))$ for $p \leq .37$. Values close to 1 indicate no favored H1.